Research Article

Cancer Epidemiology, Biomarkers & Prevention

Autoantibodies against HSF1 and CCDC155 as Biomarkers of Early-Stage, High-Grade Serous Ovarian Cancer

Amy L. Wilson[1,2], Laura R. Moffitt[1,2], Nadine Duffield[1,2], Adam Rainczuk[1,2], Tom W. Jobling[4,5], Magdalena Plebanski[3,6], and Andrew N. Stephens[1,2,5]

Abstract

Background: Tumor-directed circulating autoantibodies (AAb) are a well-established feature of many solid tumor types, and are often observed prior to clinical disease manifestation. As such, they may provide a good indicator of early disease development. We have conducted a pilot study to identify novel AAbs as markers of early-stage high-grade serous ovarian cancers (HGSOCs).

Methods: A rare cohort of patients with early (FIGO stage Ia-c) HGSOCs for IgG, IgA, and IgM-mediated AAb reactivity using high-content protein arrays (containing 9,184 individual proteins). AAb reactivity against selected antigens was validated by ELISA in a second, independent cohort of individual patients.

Results: A total of 184 antigens were differentially detected in early-stage HGSOC patients compared with all other patient groups assessed. Among the six most highly detected "early-stage" antigens, anti-IgA AAbs against HSF1 and anti-IgG AAbs CCDC155 (KASH5; nesprin 5) were significantly elevated in patients with early-stage malignancy. Receiver operating characteristic analysis suggested that AAbs against HSF1 provided better detection of early-stage malignancy than CA125 alone. Combined measurement of anti-HSF1, anti-CCDC155, and CA125 also improved efficacy at higher sensitivity.

Conclusions: The combined measurement of anti-HSF1, anti-CCDC155, and CA125 may be useful for early-stage HGSOC detection.

Impact: This is the first study to specifically identify AAbs associated with early-stage HGSOC. The presence and high frequency of specific AAbs in early-stage cancer patients warrants a larger scale examination to define their value for early disease detection at primary diagnosis and/or recurrence. *Cancer Epidemiol Biomarkers Prev; 27(2); 183–92. ©2017 AACR.*

Introduction

High-grade serous ovarian cancers (HGSOCs) are typically diagnosed at an advanced stage, and account for approximately 90% of all ovarian cancer–related deaths (1). The combination of late-stage diagnosis and the prevalence of chemoresistant disease both contribute to an overall approximately 30% 5-year survival rate, the lowest for any gynecologic tumor type. Early diagnosis, prior to extra-ovarian spread, is associated with improved survival (2); regular longitudinal screening is therefore widely accepted as the strategy of choice to reduce ovarian cancer-related mortality. Despite intensive efforts and the identification of large numbers of potential novel biomarkers of ovarian cancer (recently reviewed; refs. 3, 4), at present only CA125 and HE4 have demonstrated clinical relevance; and neither are suitable for the detection of early-stage disease (5, 6). Large-scale trials combining CA125 with transvaginal ultrasound have also failed to deliver tangible improvements in overall survival for HGSOC patients (7). There remains an unmet clinical need to identify novel disease biomarkers for use in improved early-stage diagnosis, and to monitor disease recurrence.

The release of soluble biomarkers from early-stage, microscopic HGSOC lesions is unlikely to reach measurable concentrations circulation at a sufficiently early-stage for diagnostic purposes. However, in many solid tumor types the aberrant expression, or alterations to the function, structure, or localization of proteins, can elicit an autoimmune response (8). The presence of circulating auto-antibodies (AAbs) against tumor-associated antigens (TAAs) is well documented, and occurs prior to clinical disease manifestation and is maintained throughout progression in multiple solid cancers (reviewed in ref. 9). As potential cancer biomarkers, the measurement of AAbs has several potential advantages; AAbs are stable in circulation, can recognize cancer-specific modifications to proteins that may not be immediately evident from molecular or genetic profiles, and can effectively amplify tumor-associated signals that are otherwise below detection thresholds (9). As an early and sensitive indicator of tumor growth, AAb

[1]Department of Molecular and Translational Sciences, Monash University, Victoria, Australia. [2]Centre for Cancer Research, Hudson Institute of Medical Research, Victoria, Australia. [3]Department of Immunology and Pathology, Monash University, Melbourne, Australia. [4]Obstetrics and Gynaecology, Monash Medical Centre, Clayton, Victoria, Australia. [5]Epworth Research Institute, Epworth HealthCare, Richmond, Victoria, Australia. [6]School of Health and Biomedical Sciences, RMIT, Bundoora, Victoria, Australia.

Note: Supplementary data for this article are available at Cancer Epidemiology, Biomarkers & Prevention Online (http://cebp.aacrjournals.org/).

A.L. Wilson and L.R. Moffitt contributed equally to this article.

Corresponding Author: Andrew N. Stephens, Hudson Institute of Medical Research, 27-31 Wright St Clayton, Victoria 3168, Australia. Phone: 613-8572-2686; Fax: 613-9594-7909; E-mail: Andrew.N.Stephens@hudson.org.au

doi: 10.1158/1055-9965.EPI-17-0752

measurement may therefore overcome practical limitations associated with the direct measurement of soluble TAAs. Accordingly, AAb profiling has become an attractive approach to biomarker discovery for early-stage tumor detection (10).

Diverse experimental approaches have been applied for AAb identification in multiple tumor types (recently reviewed in refs. 4, 11) including phage display, cDNA expression library analyses, reversed phase, recombinant antigen and tumor lysate arrays, and various other proteomic approaches (8, 12–14). In particular, the recent development of programmable and/or commercially available, high-content antigen arrays has facilitated the rapid profiling of AAb signatures in patient sera as a mechanism to discover new biomarkers and biomarker combinations associated with ovarian cancer (12, 15–17). However, the majority of these studies have focused on the detection of AAbs in late-stage HGSOC patients. The dynamic and location-specific nature of humoral immune responses (9) makes it unlikely that these profiles will adequately reflect events occurring early in tumor progression. Moreover, most studies do not appropriately differentiate between low- and high-grade tumors (more recently described as type I or type II, respectively) which exhibit different clinical behaviors, etiologies, and underlying molecular biology (1). Unsurprisingly, no identified AAbs have yet demonstrated suitable sensitivity, specificity, or predictive power for clinical application for the detection of early-stage HGSOC.

In this pilot study, we sought to identify circulating AAbs specifically associated with early-stage HGSOCs. Plasma samples obtained from patients diagnosed with HGSOC and stratified according to FIGO stage (stage I – early, versus stage III – late) were profiled for AAb (IgG, IA, and IgM) reactivity against commercially available Protoarray antigen arrays, displaying 9,134 individual antigens. Following the identification potential early-stage AAbs, we assessed their frequency by ELISA in a second, independent sample cohort. To our knowledge, this is the first study to focus on the identification of AAbs of multiple Ig types that are specific to early-stage HGSOCs. This pilot work provides the methodology for expanded studies to identify and validate clinically relevant biomarkers of early-stage HGSOC.

Materials and Methods

Clinical specimens

EDTA-chelated plasma samples were accessed from biobanked samples, collected prospectively from women undergoing surgery for suspected gynecologic malignancies during the period 2007–2012. All clinical samples were obtained from anesthetized patients who had undergone no prior surgical treatment or neoadjuvant chemotherapy. Healthy control samples, matched for age and menopausal status, were obtained from nonanesthetized volunteers by venipuncture. Patients were excluded if they had any prior history of cancer or gynecologic disease. Women who had undergone prior tubal ligation were also excluded. Histologic assessment of tumor type, stage and grade, presurgical CA125 measurements, age, menopausal status, preexisting conditions, and any prior history of malignancy were obtained from deidentified patient medical records. Patient details immediately relevant to this study are provided in Table 1. Measurement of serum CA125 in control samples was performed in the diagnostic pathology laboratory at the Monash Medical Centre, Melbourne, Australia. Ethical approval was obtained from the Southern Health Human Research Ethics Committee (HREC certificates #06032C, #02031B) with all participants providing prior informed written consent.

Immunoglobulin isotyping arrays

Immunoglobulin (Ig) isotype titers were determined for all individual samples using Quantibody Human Ig Isotype Array 1 (#QAH-ISO-1, RayBiotech) as described by the manufacturer. Plasma samples were diluted 1:80,000 in sample diluent, and 100 μL per sample was analyzed in triplicate. A single array incubated in sample diluent alone was used to control for nonspecific binding of the detection antibody. Dried slides were stored at room temperature and protected from light until image capture and analysis.

ProtoArray protein arrays

Proteomic profiling of antibody signatures was performed using Invitrogen ProtoArray Human Protein Microarrays v5.0 (Thermo Fisher Scientific), comprising 9,184 individual recombinant human proteins spotted in duplicate. All procedures were carried out according to the manufacturer's recommendations. Arrays were probed using pooled plasma samples diluted 1:340 in wash buffer. Fluorescent detection antibodies against human IgG, IgA, and IgM were obtained from Abcam (#ab98554 goat anti-human IgA α chain-DyLight 550; #ab98544 goat anti-human IgM μ chain-DyLight 488; #ab98622 anti IgG Fc-Dylight 650), diluted to a concentration of 1 μg/mL in wash buffer prior to use. Arrays were first incubated with anti-IgG and anti-IgM antibodies simultaneously, then washed and incubated with anti-IgA. A single array incubated in wash buffer alone was used to assess nonspecific detection–antibody binding. Dried slides were stored at room temperature and protected from light until image capture and analysis.

Array image capture and analysis

Fluorescent array signals were acquired using a Fuji FLA5100 four-channel laser scanner (FujiFilm, Tokyo) using blue (473 nm excitation, custom Cy2 emission filter), green (532 nm excitation, dual Cy3/Cy5 filter), and red (635 nm excitation, dual Cy3/Cy5 filter) imaging channels. All images were acquired at 10-μm resolution, with PMT set at 1,000 V. Quantibody arrays were imaged for green fluorescence only, while cyclic imaging was used to acquire blue, green, and red fluorescence data from Protoarrays. Array alignment, feature extraction and data normalization was performed using Phoretix Array v10.2 (TotalLab Ltd). Quantibody array data were analyzed using Quantibody Q-Analyzer software (Raybiotech), with Ig quantitation performed against an 8-point standard curve specific to each antibody isotype.

Analysis of differentially detected antigens on Protoarray arrays

Protoarray data was analyzed using Qlucore Omics Explorer v3.2 (Qlucore). Raw array data were uploaded into the workspace, $\log_2$-transformed, and collapsed according to RefSeq identification number. Average intensities were used for all comparisons, with comparisons performed separately for each of the IgG, IgA, and IgM classes. Nonspecific antigens that exhibited cross-reactivity with detection antibodies alone were removed from the analysis. Data complexity was reduced by filtering to remove all variables in the dataset with $\leq$5% variance, leaving 9,037

variables for analysis. Principal components analysis (PCA) and hierarchical clustering were used to explore the data for differentially detected, immunoreactive antigens that best defined each sample group. Discriminating antigens displayed as heatmaps were arranged by hierarchical clustering according to detection intensity, separated by Ig class and ordered by sample type.

Antigen-specific ELISA

Immunoassays for individual antigens of interest were constructed using commercially available recombinant antigens (Supplementary Table S1), corresponding to antigens of interest identified on arrays. In each case, antigens were diluted to 4 mg/mL in binding buffer ($NaHCO_3$ 100 mmol/L, N_2CO_3 33.6 mmol/L, pH 9.6), and a 100 μL volume incubated in sealed Nunc Maxisorp 96-well microplates (Thermo Fisher Scientific) overnight at 4°C with shaking (GrantBio PMS1000i shaker, 300 rpm). Serial dilutions of purified human serum IgG, IgM and IgA (Sigma Aldrich) were incubated in parallel (range 0.5–0.178 μg/mL) for the construction of standard curves. The following morning wells were washed three times in blocking buffer (1% w/v BSA, 0.05% v/v Triton X-100, NaCl 200 mmol/L in PBS), and then a 100-μL aliquot of human plasma (diluted 1:20 in blocking buffer) added to appropriate wells in triplicate. Blocking buffer alone was used in those wells containing standards. Samples were incubated at room temperature for 1 hour with shaking, followed by 3× washes as above. To detect the binding of serum Igs to the immobilized antigens, a 100-μL aliquot of anti-IgG (3 μg/mL) and anti-IgM (5 μg/mL) cocktail in ice-cold blocking buffer was added to each well and the plate incubated at room temperature with shaking for 1 hour. Following ×3 washes as above, 100 μL of anti-IgA (5 μg/mL) in blocking buffer was added and the plate incubated for a further 1 hour. All wells were then washed five times in wash buffer, and 100-μL PBS added to each prior to measurement.

Fluorescence detection was performed using a Cytation 3 MultiMode Plate Imager (BioTek Instruments Inc.). Acquisition of fluorescence intensity corresponding to IgM (485 nm excitation, 520 nm emission), IgA (550 nm excitation, 580 nm emission), and IgG (645 nm excitation, 675 nm emission) signals was performed using a fixed probe height of 6.75 mm, acquiring 200 data-points per well, and dynamic range between 100 and 80,000 units. Standard curves were constructed using Gen5.0 software v2.05 (BioTek Instruments Inc.) and individual Ig titres for each antibody type automatically determined. All assays were performed in triplicate.

Statistical analyses

Statistical analyses of immunoassay data were carried out using GraphPad PRISM (GraphPad Software). For statistical purposes, data was log transformed to approximate normality. Significance was determined using one-way ANOVA and Bonferroni *post hoc* test, with pairwise comparisons performed using Student *t* test. For groups with significantly different variance, Welch correction was applied. Results of $P \leq 0.05$ were considered significant. ROC analysis was performed on log-transformed data using R open source software according to the method of Palmer (18), with healthy controls scaled to have a mean of zero and a variance of one. Markers were ranked according to specificity at defined sensitivity (90%, 95%, or 98%), with early-stage cancer cases ($n = 10$) compared with all controls ($n = 30$ women with no disease or benign disease). To restrict bias in marker performance, statistical fitting was not used. The R script is provided in Supplementary Data S2.

Results

Sample characteristics and antigen identification strategy

The overall strategy for autoantigen identification and validation is presented in Fig. 1A. Individual plasma samples were randomly assigned into "discovery" or "validation" groups, and antigen array experiments performed using pooled discovery group samples to provide an averaged biological measurement. We have previously established this as a cost-effective strategy for proteomic discovery studies (19). Antigens detected by protein arrays were independently confirmed by ELISA, and then retested on individual samples in the validation cohort to determine the prevalence of autoantibodies in patient's plasma.

Inclusion criteria were tightly controlled to provide age- and pathology-matched groups for investigation (Table 1). All samples were obtained from patients at first surgical presentation, prior to any chemotherapy, and were matched for age and menopausal status. Patients were excluded if they had any prior history of gynecologic disease or cancer, and were additionally excluded from control groups if they had a known predisposition (genetic or familial history) of breast or ovarian cancer. Women diagnosed with benign cystadenoma (representing ∼20% of all ovarian neoplasms, typically exhibiting simple cystic structure) or benign cystadenofibroma (representing ∼1.7% of ovarian neoplasms, and often exhibiting complex architecture and vascularization; refs. 20, 21) were included as confounding groups to reduce potential false positives. There were no significant differences in immunoglobulin (Ig) content or subtypes among the samples investigated, nor in average age of the cohort, and, as expected, CA125 was significantly elevated in both early- and late-stage cancer patients relative to all other groups (Supplementary Fig. SF1).

Antibody signatures discriminating between healthy, benign, and malignant conditions

We first assessed normalized Protoarray data using PCA to determine whether antibody signatures differentiated between samples representing (i) no disease, (ii) women with benign ovarian disease, or (iii) women with malignant disease. In addition to IgG profiling, we also assessed IgM (representing early immune response, prior to affinity maturation and class switching; ref. 22) and IgA (representing mucosal surface immunity; ref. 23) responses. Combining all differences (i.e., IgG, IgA, and IgM reactive antigens) identified between disease groups yielded a total of 1,389 antigens that discriminated between no disease, benign disease, or cancers; 96 antigens of these antigens reacted with multiple Ig types. These 1,389 antigens were further restricted by pairwise comparison to include only those showing at least a 2-fold difference ($P \leq 0.05$) between groups (Fig. 1B; Supplementary Table S3). IgM and IgG reactivity was dominant, with antigens recognized by IgA comprising only approximately 15% of the total differences observed. In contrast, we observed substantially fewer differentiating antigens in patients with benign disease; only 69 antigens were significantly different in this group compared with healthy women (Supplementary Table S3), of which approximately 90% were recognized by IgG.

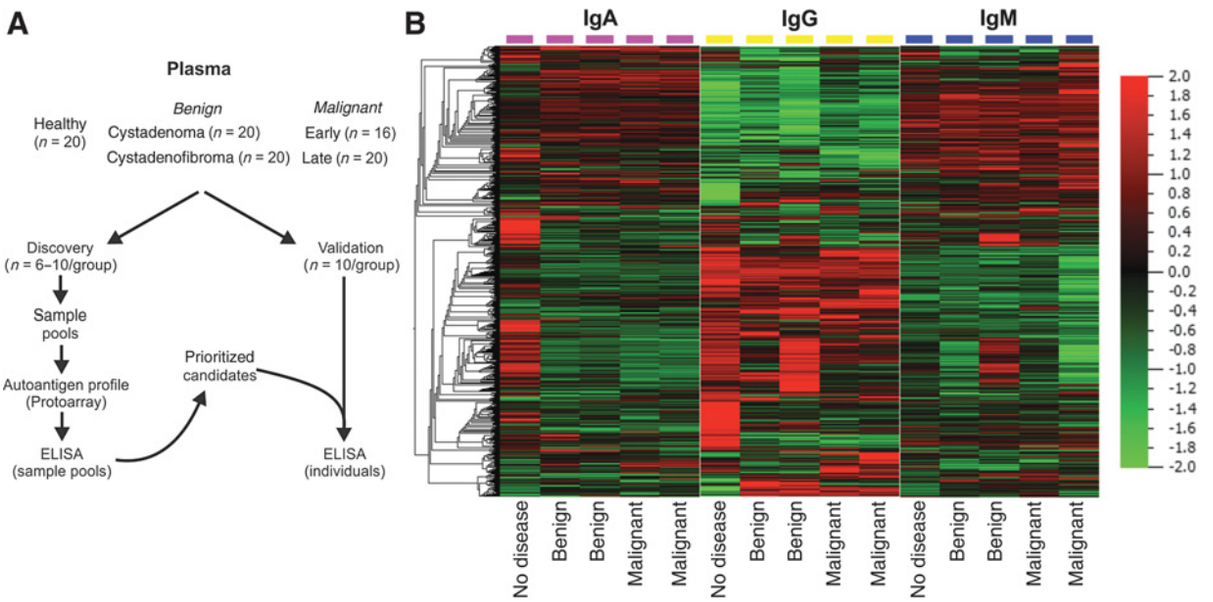

Figure 1.

A, Autoantigen discovery and validation strategy. Plasma samples were randomly divided into two cohorts ("discovery" and "validation"); all disease subgroups had $n = 10$, except for the early-stage cancer discovery group ($n = 6$). Disease sub-groups in the discovery cohort were pooled and used to probe Protoarray protein microarrays for the presence of AAbs against cross-reacting antigens. ELISA was used to validate changes in the discovery pools. Selected antigens were then re-examined by ELISA in individual patient plasma samples from the validation cohort. **B,** Identification of antigens discriminating between groups. Heatmap of antigen detection intensity differentiating between disease states. Individual genes are ordered by hierarchical clustering; samples are ordered by IgG type as indicated. Relative intensity scale is shown.

Comparing our dataset to several similar array studies (15–17, 24), we identified 40 common cancer-specific antigens (Supplementary Table S4) confirming the validity of the approach. As expected, these were largely IgG-mediated; no other studies have investigated the global contribution of IgA to ovarian cancer immune signatures. We also identified five autoantigens associated specifically with benign neoplasms (BYSL, PCBP1, MAGEB2, RAB11B, and ATG4A) that had been previously suggested as potential cancer-associated antigens (15, 16), highlighting the importance of including these confounding samples to overcome false positives in the noncancer setting.

AAb signatures discriminating between localized versus disseminated disease

The exposure, presentation, and recognition of tumor antigens is likely to vary according to tumor localization and progression (25); however, no studies have specifically explored the presence of autoimmune signatures in patients with early-stage compared with high-grade disease. Among those variables associated with malignancy, a total of 184 differences were specific to the early-stage cancer group (FIGO grade 3, stages Ia–c) with 19 antigens recognized by multiple Ig types (Supplementary Table S3). While IgG reactivity was dominant, IgA-reactive antigens were substantially more common in early-stage plasma samples than was observed for late-stage patients and comprised approximately 37% of differences detected (Fig. 2A). Among these were 17 "overlapping" antigens detected in both the early- and late-stage cancer groups (13 recognized by IgG, 4 by IgA), suggesting that while some antigens are dynamically presented or recognized, others may persist throughout disease progression (Table 2).

Enrichment for the cellular distribution of all identified antigens was assessed by Gene Ontology (GO) term, according to disease, stage, and Ig type (Fig. 2B). Cytoskeletal, nuclear, and

Table 1. Summary of sample cohort characteristics

					Discovery cohort			Validation cohort		
Group	Pathology	Grade	Stage	Menopausal status	# Patients	Median age (IQR)	Median CA125 (IQR)	# Patients	Median age (IQR)	Median CA125 (IQR)
Healthy	None	n/a	n/a	post	$n = 10$	59.5 (59–60)	9.5 (7–12.5)	$n = 10$	59.5 (56–65.5)	11.5 (8–15)
Benign A	Serous cystadenoma	n/a	n/a	post	$n = 10$	62 (57–73)	34 (11–50.5)	$n = 10$	59.5 (56–62)	18.5 (12–36)
Benign B	Serous cystadenofibroma	n/a	n/a	post	$n = 10$	70 (57.5–75)	14 (12–16)	$n = 10$	68 (62–70)	10 (9–14)
Early ($n = 6$)	Serous papillary carcinoma	3	I (a-c)	post	$n = 6$	56 (55.5–56)	130.5 (100–243)	$n = 10$	57 (53–69.5)	113.5 (28–199)
Late ($n = 10$)	Serous papillary carcinoma	3	IIIc	post	$n = 10$	59.5 (56–65)	1583.5 (681–3,093)	$n = 10$	60 (59–64.5)	1,004 (488–1,843)

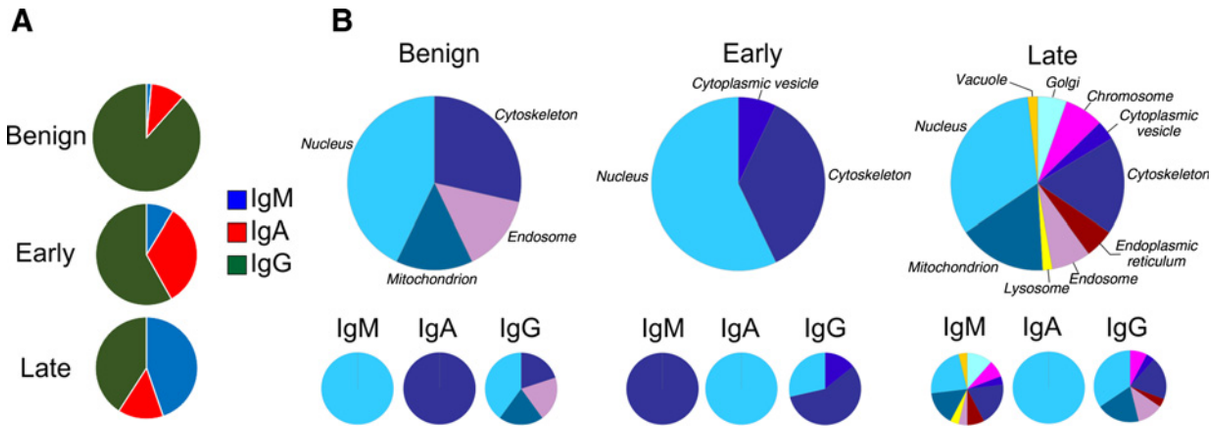

Figure 2.

Ig type and gene ontology localization of antigens associated with benign or malignant disease. **A,** Percentage of Ig type reactivity according to disease state. **B,** Antigen localization (top) and percentage of contributing antibody type (bottom) according to GO term in benign, early- or late-stage tumors.

mitochondrial antigens were over-represented in all disease states; while endosomal or cytoplasmic vesicle antigens were identified in benign or early cancer, respectively. Late-stage antigens were far more diverse in their cellular localizations (Fig. 2B), likely reflecting increased exposure of intracellular antigens in the apoptotic/necrotic cancer environment. Interestingly, cellular localization according to GO annotation differed considerably between Ig types and disease status. IgA-reactive antigens were generally nuclear in cancers, but cytoplasmic in benign disease; in contrast, IgM-reactive antigens in early-stage cancer were cytoplasmic, but were nuclear in benign disease (Fig. 2B).

Functional enrichment analysis of cancer antigens

To identify how differences in antigen recognition might reflect biological function, enrichment analysis was performed using Ingenuity Pathways Analysis (IPA) software. Differentially detected antigens (Supplementary Table S3) were uploaded and examined in benign, early-stage and late-stage specific groupings. Unsurprisingly, canonical DNA damage–induced 14-3-3 gamma signaling was significantly over-represented ($P \leq 0.001$) within the cancer antigen dataset (Supplementary Table S5). Cancer antigens in general were enriched ($P \leq 10^{-5}$) for processes involving cell cycle, gene expression, and DNA repair; cellular organization, function, and movement; and metabolic processes including lipid, amino acid, and other small-molecule biochemistry (Supplementary Table S5). When separated according to stage, both early- and late-stage antigens were enriched for cancer, organismal injury, and cell death/survival–related processes. Cell–cell signaling, cellular assembly, and inflammatory response were more highly enriched among late-stage cancer antigens; contrastingly, cell cycle, growth, and proliferation were all over-represented among the early cancer antigens (Supplementary Table S5). No significant functional enrichment was observed among benign-specific antigens, although two cancer-related

Table 2. Identified antigens common to both early- and late-stage cancers

			Early		Late	
GenBank #	**Protein name**	**Ig type**	***P***	**Fold**	***P***	**Fold**
NM_016638.1	ADP-ribosylation factor-like protein 6-interacting protein 4	IgA	0.022	2.8	0.030	2.4
BC001396.1	Chromosome 9 open reading frame 32 (C9orf32)	IgG	0.040	−2.4	0.050	−2.2
NM_001311.2	Cysteine-rich protein 1	IgG	0.004	2.3	0.003	2.8
NM_017541.2	Beta-crystallin S	IgG	0.010	3.5	0.011	3.3
NP_004084.1	EphrinB2/EFNB2 Protein	IgG	0.015	−2.9	0.027	−2.2
		IgA	0.038	2.0	n/a	n/a
NM_207009.2	Family with sequence similarity 45, member A (FAM45A), mRNA	IgG	0.038	−2.0	0.011	3.8
NM_145269.1	Protein FAM92A1	IgA	0.014	−2.3	0.018	−2.1
NM_173558.2	FYVE, RhoGEF and PH domain-containing protein 2	IgG	0.038	−2.3	0.050	−2.0
BC034146.1	Immunoglobulin kappa variable 1–5 (IGKV1-5)	IgG	0.013	−3.6	0.033	−2.2
NM_207350.1	Similar to FRG1 protein (FSHD region gene 1 protein) (MGC72104)	IgG	0.019	4.1	0.013	5.7
BC008624.1	cDNA clone MGC:18299 IMAGE:4179890, complete cds	IgG	0.044	2.7	0.044	2.7
		IgA	0.033	4.3	n/a	n/a
NM_002625.1	6-phosphofructo-2-kinase/fructose-2,6-biphosphatase 1	IgG	0.043	2.5	0.032	2.9
NP_006262.1	S100A1 Protein	IgG	0.014	−3.3	0.015	−3.2
BC000522.1	Serpin peptidase inhibitor, clade F (alpha-2 antiplasmin, pigment epithelium derived factor), member 1 (SERPINF1)	IgG	0.029	−2.4	0.042	−2.1
BC011234.1	Survival motor neuron domain containing 1 (SMNDC1)	IgG	0.040	−2.4	0.039	−2.4
NM_022827.2	Spermatogenesis associated 20 (SPATA20)	IgG	0.022	−2.2	0.042	−2.6
		IgA	0.035	−2.8	n/a	n/a
NM_004179.1	Tryptophan hydroxylase 1 (tryptophan 5-monooxygenase) (TPH1)	IgA	0.003	3.4	0.005	2.3

networks were identified suggesting some enrichment of functions related to cell growth, proliferation, and survival (Supplementary Table S5).

In keeping with the observed enrichment for cytoskeletal proteins, early IgM-reactive antigens were associated with biological processes related to cell morphology and movement including actin polymerization, stress fiber formation and branching, while late-stage IgM-reactive antigens were related to proliferation, immune function, and secretion (Supplementary Table S5). Early IgG-reactive antigens were associated with apoptosis, adhesion, morphogenesis, and malignancy, while late-stage IgG-reactive antigens were enriched for proliferation. In contrast, early IgA-reactive antigens were linked with cell damage, cell death, and posttranslational modification, while late-stage IgAs were enriched for processes involved in cell clustering. The data suggest that substantially different biological processes are targeted by the different Ig types, and that this process is dynamic, according to the evolution and progression of high-grade serous ovarian tumors (26).

Functional autoantibody networks according to disease stage

Network analyses were performed to identify direct relationships between the identified antigens. In both the early- and late-stage cancer groups, several causal networks strongly suggested the involvement of ERK1/2, p38MAPK, NFκB, and IFN signaling (Supplementary Table S5). Networks associated with early-stage disease were most notably involved inflammatory cytokine signaling and increased metabolic activity, while those identified in late-stage disease tended to cluster around key signaling networks (e.g., ERK1/2, NFκB). The assignment of genes to these functional networks corresponded with strong correlations ($\geq$97% Pearson correlation) in their detection on antigen arrays.

Among the IgG-reactive cancer antigens identified, linear correlation analysis revealed two subgroupings of antigens that displayed similar patterns of detection within cancer groups (Pearson coefficient = 0.97). Collectively, these correlated antigens formed potential "linking" networks suggesting functional relationships between early- and late-stage diseases (Fig. 3A). Each of these networks were investigated further for potential functional relationships that might link antigen recognition between localized and disseminated disease (Supplementary Table S5). Linking network 1 was associated with inflammation, and was enriched for processes involving movement, growth, proliferation, and morphology. In contrast, linking network 2 was associated with metabolism and molecular transport. Enriched functions included cell movement and morphology, cell cycle, and cell–cell signaling. Genes contained within these networks were strongly discriminatory between cancer versus all other sample groups (Fig. 3B).

Validation of selected autoantigens by ELISA

To validate differences in selected antigen reactivity, we first used ELISA to confirm changes observed in the discovery pools. Antigen selection was limited to those antigens for which recombinant or purified protein, homologous to those printed on Protoarrays, could be commercially sourced. In total, we confirmed 19 of 27 antigen-specific changes by ELISA (Supplementary Table S6). Among those validated were several antigens previously identified in similar array experiments, including GMEB1, HMGA1, PFKFB1, and BC008624.1 (16, 24).

To establish the prevalence of AAbs in individual patients, the six antigens with the greatest fold difference detected between sample groups (BAG5, CCDC155, CEP72, GMEB1, HSF1, and SEC23IP) were reevaluated among individual patients (n = 10/group) from the "validation" cohort. The prevalence of autoantibodies against BAG5, CEP72, GMEB1, and SEC23IP was highly variable among individual patients; none of these were validated as potential biomarkers of ovarian cancer.

In contrast, two antigens (CCDC155 and HSF1) were significantly elevated in the majority of early-stage patients, in

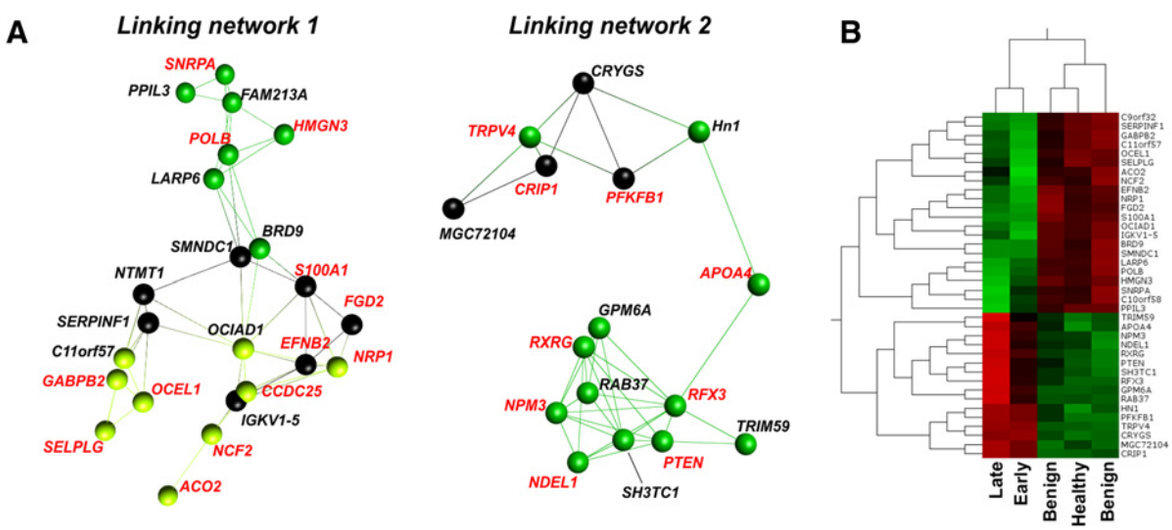

Figure 3.

Antigen reactivity networks linking early- with late-stage disease. Two strongly correlated expression networks (**A**) were identified that displayed overlapping antigen reactivity between early- and late-stage disease. Light green, early-stage; dark green, late stage; black, overlapping. **B,** Heatmap of IgG-reactive genes in linking networks 1 and 2. Genes and samples are ordered by hierarchical clustering.

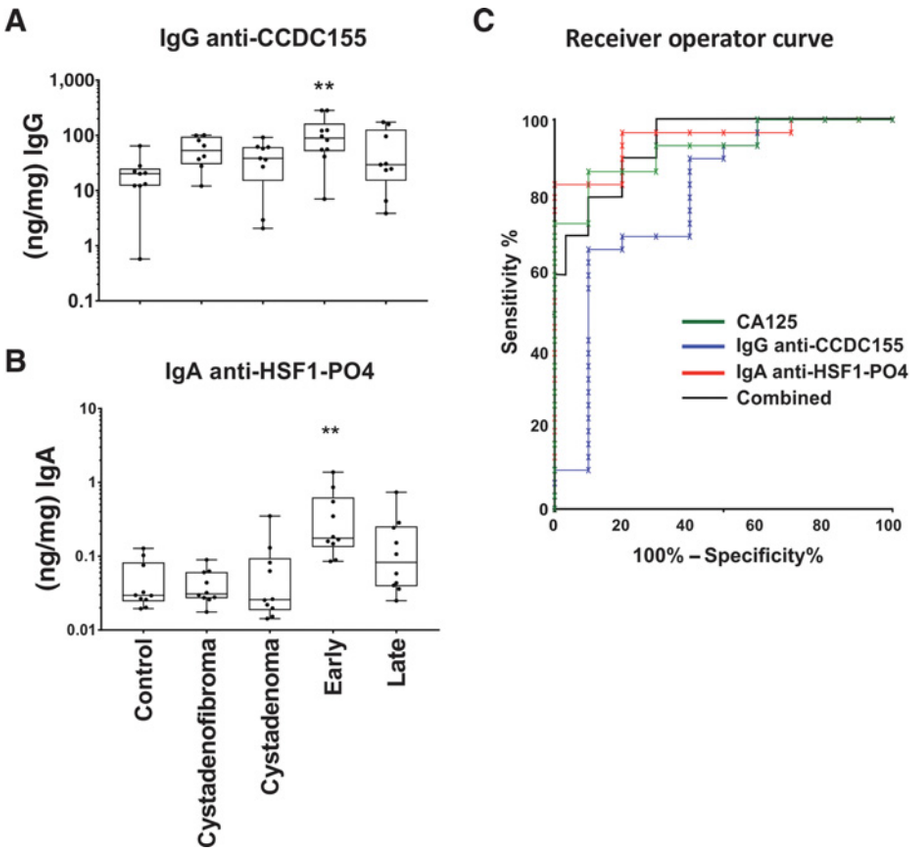

Figure 4.

Validation of autoantibodies against CCDC155 and HSF1 in the independent validation cohort by ELISA. Individual samples ($n = 10$/group) from the validation cohort were analysed for reactivity of (**A**) plasma IgG against CCDC155, or (**B**) plasma IgA against HSF1-PO4. Titres were adjusted for total IgG or IgA titre, respectively. **, $P \leq 0.01$. **C,** ROC analysis was performed on early-stage cancer samples ($n = 10$) *versus* all control and benign disease samples ($n = 30$). Calculated sensitivity/specificity for each marker and marker combination are provided in Supplementary Table S7.

agreement with data from the discovery set. IgG-specific reactivity against CCDC155 was significantly elevated ($P = 0.0013$) in patients with early-stage disease compared with healthy controls (Fig. 4A). Similarly, IgA-specific reactivity against phosphorylated HSF1 was elevated ($P = 0.0007$) in the same patient group (Fig. 4B). Interestingly, AAbs were specific for the phosphorylated form of HSF1, and did not discriminate between disease states when the nonphosphorylated variant was tested (Supplementary Table S6). There was no correlation observed between either CCDC155 or HSF1 reactivity with CA125 (Pearson coefficient).

ROC analyses were carried out to determine the potential diagnostic efficacy of each marker (Fig. 4C; Supplementary Table S7). Statistical fitting was not used due to the small size of the dataset. For the detection of early-stage disease, the best performing marker was HSF1 with sensitivity/specificity of 95%/80% (AUC 0.95) (Fig. 4C; Supplementary Table S7); this was comparatively higher that of CA125, which gave sensitivity/specificity of 95%/40% (AUC 0.93). Single measurement of anti-CCDC155 antibody performed similarly to CA125, with a sensitivity/specificity of 95%/40% (AUC 0.8). Multiple marker combinations at 95% sensitivity did not increase the overall specificity of early-stage HGSOC detection compared with HSF1 alone. However, at a sensitivity of 98% there was improved specificity using the combination of all three markers (Supplementary Table S7), suggesting a potentially additive effect of the combined measurements.

For the differentiation of all cancers from all controls, the combination of HSF1 – CA125 provided better discrimination than CA125 alone; CCDC155 did not reach significance in this comparison. Similarly, neither HSF1 nor CCDC155 reached significance for the differentiation of late-stage disease, where CA125 was clearly the best performed (sensitivity/specificity 99%/100%; Supplementary Table S7). Thus, autoantibodies against HSF1 provided better diagnostic efficacy than CA125 alone for the detection of early-stage disease patients in this small dataset, and the three-marker combination potentially provided improved diagnostic efficacy at high sensitivity for patients with early-stage HGSOCs.

Discussion

In this pilot study, we sought to determine whether AAb profiles could discriminate between early-stage HGSOCs from nonmalignant controls. We restricted our focus to high-grade (type II) epithelial tumors, as these account for approximately 90% of all ovarian cancer-related mortality (1) and therefore represent a patient group that would benefit substantially from early diagnosis. These tumors exhibit substantially different underlying molecular biology and clinical behaviors to low-grade (type I) tumors (1), and these distinct disease types are unlikely to parallel each other in terms of antigen presentation. Nevertheless, few autoantibody discovery studies have made the distinction between disease subsets.

A major limitation for studies focused on early-stage HGSOCs is their rarity of diagnosis, primarily due to their asymptomatic nature and aggressive behavior (1). Indeed, our cohort of 16 patients with FIGO stage I HGSOC was collected

over 6 years, and represents approximately 1% of the total number of HGSOC samples collected during that time. To maximize the potential use of these rare samples, we performed discovery experiments using pooled samples followed by independent validation in a separate cohort of individuals. This provides an efficient and cost-effective approach to biomarker discovery and validation (19), and reduces the use of precious and rare clinical material. Retrospective power analyses suggested that 10 individuals per group was sufficient to detect significant changes in this study. Moreover, the substantial overlap in identified antigens between this and other autoantigen profiling studies (8, 12, 16, 17, 24, 27, 28) suggests that this approach is suitable for the investigation of cancer autoantigens in plasma. To our knowledge, no previous studies have evaluated autoimmune signatures in patients specifically associated with early-stage HGSOCs.

Humoral immune responses are both disease-dependent and location specific; accordingly, both antigen specificity and recognition according to Ig type differed between disease states and the stage of disease dissemination. Antigens themselves were derived from multiple cellular compartments, with the greatest diversity evident for advanced-stage cancer patients. This most likely reflected an increasing level of antigen exposure at different stages of progression, with extensive inflammation contributing to increased levels of apoptotic/necrotic cell death and subsequent recognition of intracellular antigens (29). Several TAAs were also recognized across both early- and late-stage cancer patient groups and were strongly correlated in their abundance and biological functions. In keeping with the adaptive nature of humoral immunity (9), our data suggest that an antigen-specific immune response may be maintained across progressive disease stages; and that the disease-specific recognition of TAAs depends on their identity, cellular origins, and the immune-specific context of their recognition.

To provide a complete profile of circulating AAbs in ovarian cancer patients, secretory IgA- and IgM-mediated responses were examined for the first time in addition to IgG. Surprisingly, IgA AAbs were significantly more abundant in early-stage than late-stage disease, suggesting they may be useful early indicators of malignancy. Both IgA and IgM are the main humoral mediators of mucosal immunity (30–32). Local immune cells associated with mucosal surfaces in the upper female reproductive tract maintain immune surveillance and establish tolerance for sperm and the developing embryo (33), and while IgGs in the genital tract are generally derived from circulation, IgA is produced locally (34, 35). IgA-positive cells in fallopian tube mucosae increase in response to local inflammation (36, 37), and both IgA and secretory component have been found in patients with adenocarcinomas of the endocervix, endometrium, and fallopian tubes (38). As the majority of HGSOCs are suggested to evolve from serous tubal intraepithelial carcinoma (STIC) lesions in the fallopian tube (1), IgA autoantibodies may play an important role in early tumor recognition.

We identified and validated AAbs against two antigens, HSF1 and CCDC155, as potential new biomarkers of early-stage HGSOC. Heat shock transcription factor 1 (HSF1) is a master regulator of the heat shock response, and drives the transcription of multiple stress response genes. Previous work has established that IgA AAbs against HSP27, a downstream target of activated, phosphorylated HSP1, are found in women with gynecologic malignancies, particularly in women with ovarian cancer (~75%; ref. 35). Notably, HSF1 is overexpressed in a significant proportion of ovarian cancer patients (39, 40). Knockdown or knockout of HSF1 results in decreased proliferation, decreased migration, and increased apoptosis in ovarian cancer cells; and prolongs survival time in xenograft models of ovarian cancer (39, 40). The loss of HSF1 also alters ovarian cancer spheroid morphology *in vitro*, and the expression of EMT markers fibronectin, SNAIL, SLUG, and TWIST1; thus, HSF1 has been proposed as a potential anticancer therapeutic target (39, 40). Indeed, recent work has identified that a nucleoside analog Ly101-4B elicits efficient inhibition of HSF1 expression, and exerts potent anticancer activity both *in vitro* and *in vivo* (41).

Importantly, our data showed that circulating autoantibodies recognized only the phosphorylated, activated form of HSF1 (and not the inactive, nonphosphorylated form). HSF1 contains multiple phosphorylation domains, whose occupancy controls the expression of HSPs (42). Recent studies suggested that the presence of activated HSF1^{pSer326} was associated with poor prognosis and reduced overall survival in ovarian cancer patients (42). Moreover, increased levels of HSF1^{pSer326} were associated with the ALDE1^{high} stem-like population (CSCs). HSF1 knock-down decreased the overall number of ALDE1^{high} CSCs, and inhibited their ability to form spheroids *in vitro* (42). Early overexpression and/or activation of HSF1 may therefore induce an AAb response, providing a potential marker for tumor detection. Further analysis of the role of HSF1 in ovarian cancers is therefore warranted.

We also identified coiled-coil domain containing 155 (CCDC155; KASH5; Nesprin-5) as a potential cancer-associated autoantigen. CCDC155 is a member of the Klarsicht, ANC-1, and Syne Homology (KASH) family of mammalian dynein–binding proteins, that participate in mechanical connections between the nuclear envelope and actin cytoskeleton (43–45). KASH proteins play important roles in nuclear migration and positioning during cell cycle, signal transduction, and DNA repair and in the regulation of invadopodia function in tumor cells *in vitro* (46, 47). As part of the SUN1 LINC complex, CCDC155 controls the progression of meiosis in germ cells; CCDC155-deficient mice (both male and female) exhibit meiotic arrest, spindle abnormalities, and defects in homologous chromosome pairing (44, 45). CCDC155 also exhibits haplotype-dependent, allele-specific methylation (48), which is tissue-type specific; notably, several other nesprins can be found as tissue-specific variants (43). The recognition of CCDC155 as a cancer-associated antigen could therefore arise as a consequence of epigenetic changes occurring in ovarian cancer cells (49). No studies have evaluated the potential contribution of CCDC155 to ovarian cancer.

Similar to other AAb studies (e.g., refs. 16, 17), we experienced a high attrition rate when attempting to validate biomarker status using an alternative detection platform. Indeed, only 2 of 27 antigen-specific AAbs identified could be confirmed in individual patients by ELISA. Notwithstanding biological variability within the population, technical limitations also hamper efforts to identify and validate biomarkers, particularly when transferring between detection platforms. For example, the inability to validate specific markers can result from differences in sensitivity or robustness of measurement offered by different platforms or, for example, the failure to present epitopes in an appropriate conformation when moving to an ELISA format, potentially resulting in an absence of reactivity and/or nonspecific cross-reactivity (28). A further

limitation, not often highlighted, lies in the binary nature of ELISA. The single endpoint of ELISA-based testing does not account for the likelihood that circulating autoantibodies may be polyclonal in nature (50). As a consequence, the binding of multiple antibody species to a single antigen may mask *bona fide* specificity; alternately, competition for binding sites may also alter reactivity profiles. The high failure rate experienced in this and other similar studies (16, 17) may therefore reflect an inability to reliably detect and quantify specific biomarkers, rather than their absence.

Our pilot data have identified AAb signatures linked with early-stage HGSOC, and validated two autoreactive antigens (CCDC155 and HSF1) that may be useful as markers of early-stage disease. Ongoing validation studies in a larger cohort are now required to fully assess their utility as biomarkers for the detection of primary or recurrent ovarian cancer.

Disclosure of Potential Conflicts of Interest

M. Plebanski serves as the director of PX Biosolutions. No potential conflicts of interest were disclosed by the other authors.

Authors' Contributions

Conception and design: M. Plebanski, A.N. Stephens
Development of methodology: L.R. Moffitt, A.N. Stephens
Acquisition of data (provided animals, acquired and managed patients, provided facilities, etc.): A.L. Wilson, L.R. Moffitt, N. Duffield, T.W. Jobling, A.N. Stephens
Analysis and interpretation of data (e.g., statistical analysis, biostatistics, computational analysis): A.L. Wilson, L.R. Moffitt, A.N. Stephens
Writing, review, and/or revision of the manuscript: A.L. Wilson, L.R. Moffitt, A. Rainczuk, M. Plebanski, A.N. Stephens
Administrative, technical, or material support (i.e., reporting or organizing data, constructing databases): A.L. Wilson, M. Plebanski
Study supervision: A. Rainczuk, M. Plebanski, A.N. Stephens

Acknowledgments

This work was supported by the Victorian Government's Operational Infrastructure Support Program. Funding support was provided by the National Health and Medical Research Council of Australia (Project #1099375) and the Ovarian Cancer Research Foundation of Australia (https://ocrf.com.au/). M. Plebanski is the recipient of a Senior NHMRC Fellowship. Clinical samples were accessed through the OCRF-sponsored Ovarian Cancer Tissue Banking program.

We thank Ms. Rhiannon Dudley and Ms. Nicole Fairweather for their assistance with clinical sample collection and associated data management. Hudson Institute data audit #9999389.

The costs of publication of this article were defrayed in part by the payment of page charges. This article must therefore be hereby marked *advertisement* in accordance with 18 U.S.C. Section 1734 solely to indicate this fact.

Received August 15, 2017; revised October 23, 2017; accepted November 9, 2017; published OnlineFirst November 15, 2017.

References

1. Kurman RJ, Shih Ie M. The dualistic model of ovarian carcinogenesis: revisited, revised, and expanded. Am J Pathol 2016;186:733–47.
2. Siegel R, Ma J, Zou Z, Jemal A. Cancer statistics, 2014. CA Cancer J Clin 2014;64:9–29.
3. El Bairi K, Kandhro AH, Gouri A, Mahfoud W, Louanjli N, Saadani B, et al. Emerging diagnostic, prognostic and therapeutic biomarkers for ovarian cancer. Cell Oncol 2017;40:105–18.
4. Shi JX, Qin JJ, Ye H, Wang P, Wang KJ, Zhang JY. Tumor associated antigens or anti-TAA autoantibodies as biomarkers in the diagnosis of ovarian cancer: a systematic review with meta-analysis. Expert Rev Mol Diagn 2015;15:829–52.
5. Badgwell D, Bast RC Jr. Early detection of ovarian cancer. Dis Markers 2007;23:397–410.
6. Moore RG, McMeekin DS, Brown AK, DiSilvestro P, Miller MC, Allard WJ, et al. A novel multiple marker bioassay utilizing HE4 and CA125 for the prediction of ovarian cancer in patients with a pelvic mass. Gynecol Oncol 2009;112:40–6.
7. Jacobs IJ, Menon U, Ryan A, Gentry-Maharaj A, Burnell M, Kalsi JK, et al. Ovarian cancer screening and mortality in the UK Collaborative Trial of Ovarian Cancer Screening (UKCTOCS): a randomised controlled trial. Lancet 2016;387:945–56.
8. Karabudak AA, Hafner J, Shetty V, Chen S, Secord AA, Morse MA, et al. Autoantibody biomarkers identified by proteomics methods distinguish ovarian cancer from non-ovarian cancer with various CA-125 levels. J Cancer Res Clin Oncol 2013;139:1757–70.
9. Zaenker P, Gray ES, Ziman MR. Autoantibody production in cancer–the humoral immune response toward autologous antigens in cancer patients. Autoimmun Rev 2016;15:477–83.
10. Dudas SP, Chatterjee M, Tainsky MA. Usage of cancer associated autoantibodies in the detection of disease. Cancer Biomarkers 2010; 6:257–70.
11. Zhu Q, Liu M, Dai L, Ying X, Ye H, Zhou Y, et al. Using immunoproteomics to identify tumor-associated antigens (TAAs) as biomarkers in cancer immunodiagnosis. Autoimmun Rev 2013;12:1123–8.
12. Hudson ME, Pozdnyakova I, Haines K, Mor G, Snyder M. Identification of differentially expressed proteins in ovarian cancer using high-density protein microarrays. Proc Natl Acad Sci U S A 2007;104:17494–9.
13. Ehrlich JR, Tang L, Caiazzo RJ Jr, Cramer DW, Ng SK, Ng SW, et al. The "reverse capture" autoantibody microarray: an innovative approach to profiling the autoantibody response to tissue-derived native antigens. Methods Mol Biol 2008;441:175–92.
14. Chatterjee M, Mohapatra S, Ionan A, Bawa G, Ali-Fehmi R, Wang X, et al. Diagnostic markers of ovarian cancer by high-throughput antigen cloning and detection on arrays. Cancer Res 2006;66:1181–90.
15. Gnjatic S, Wheeler C, Ebner M, Ritter E, Murray A, Altorki NK, et al. Seromic analysis of antibody responses in non-small cell lung cancer patients and healthy donors using conformational protein arrays. J Immunol Methods 2009;341:50–8.
16. Anderson KS, Cramer DW, Sibani S, Wallstrom G, Wong J, Park J, et al. Autoantibody signature for the serologic detection of ovarian cancer. J Proteome Res 2015;14:578–86.
17. Katchman BA, Chowell D, Wallstrom G, Vitonis AF, LaBaer J, Cramer DW, et al. Autoantibody biomarkers for the detection of serous ovarian cancer. Gynecol Oncol 2017;146:129–36.
18. Palmer C, Duan X, Hawley S, Scholler N, Thorpe JD, Sahota RA, et al. Systematic evaluation of candidate blood markers for detecting ovarian cancer. PLoS One 2008;3:e2633.
19. Rainczuk A, Condina M, Pelzing M, Dolman S, Rao J, Fairweather N, et al. The utility of isotope-coded protein labeling for prioritization of proteins found in ovarian cancer patient urine. J Proteome Res 2013;12:4074–88.
20. Cho SM, Byun JY, Rha SE, Jung SE, Park GS, Kim BK, et al. CT and MRI findings of cystadenofibromas of the ovary. Eur Radiol 2004;14:798–804.
21. Alcazar JL, Errasti T, Minguez JA, Galan MJ, Garcia-Manero M, Ceamanos C. Sonographic features of ovarian cystadenofibromas: spectrum of findings. J Ultrasound Med 2001;20:915–9.
22. Hoyer BF, Radbruch A. Protective and pathogenic memory plasma cells. Immunol Lett 2017;189:10–2.
23. Heineke MH, van Egmond M. Immunoglobulin A: magic bullet or Trojan horse? Eur J Clin Invest 2017;47:184–92.
24. Gunawardana CG, Memari N, Diamandis EP. Identifying novel autoantibody signatures in ovarian cancer using high-density protein microarrays. Clin Biochem 2009;42:426–9.
25. Dunn GP, Old LJ, Schreiber RD. The immunobiology of cancer immunosurveillance and immunoediting. Immunity 2004;21:137–48.

26. Zhang L, Conejo-Garcia JR, Katsaros D, Gimotty PA, Massobrio M, Regnani G, et al. Intratumoral T cells, recurrence, and survival in epithelial ovarian cancer. N Engl J Med 2003;348:203–13.
27. Ali-Fehmi R, Chatterjee M, Ionan A, Levin NK, Arabi H, Bandyopadhyay S, et al. Analysis of the expression of human tumor antigens in ovarian cancer tissues. Cancer Biomark 2010;6:33–48.
28. Murphy MA, O'Connell DJ, O'Kane SL, O'Brien JK, O'Toole S, Martin C, et al. Epitope presentation is an important determinant of the utility of antigens identified from protein arrays in the development of autoantibody diagnostic assays. J Proteomics 2012;75:4668–75.
29. Kourtzelis I, Rafail S. The dual role of complement in cancer and its implication in anti-tumor therapy. Ann Transl Med 2016;4:265.
30. Brandtzaeg P. Mucosal immunity in the female genital tract. J Reprod Immunol 1997;36:23–50.
31. Kutteh WH, Hatch KD, Blackwell RE, Mestecky J. Secretory immune system of the female reproductive tract: I. Immunoglobulin and secretory component-containing cells. Obstet Gynecol 1988;71:56–60.
32. Kutteh WH, Mestecky J. Secretory immunity in the female reproductive tract. Am J Reprod Immunol 1994;31:40–6.
33. Lee SK, Kim CJ, Kim DJ, Kang JH. Immune cells in the female reproductive tract. Immune Netw 2015;15:16–26.
34. Wang Y, Ben K, Cao X, Wang Y. Transport of anti-sperm monoclonal IgA and IgG into murine male and female genital tracts from blood. Effect of sex hormones. J Immunol 1996;156:1014–9.
35. Korneeva I, Bongiovanni AM, Girotra M, Caputo TA, Witkin SS. IgA antibodies to the 27-kDa heat-shock protein in the genital tracts of women with gynecologic cancers. Int J Cancer 2000;87:824–8.
36. Kutteh WH, Blackwell RE, Gore H, Kutteh CC, Carr BR, Mestecky J. Secretory immune system of the female reproductive tract. II. Local immune system in normal and infected fallopian tube. Fertil Steril 1990;54:51–5.
37. Arraztoa JA, Rocha A, Varela-Nallar L, Velasquez L, Toro V, Cardenas H, et al. IgA in the lumen of the human oviduct is not related to the menstrual cycle but increases during local inflammation. Fertil Steril 2002;77:633–4.
38. Lee YS, Raju GC. Expression of IgA and secretory component in the normal and in adenocarcinomas of Fallopian tube, endometrium and endocervix. Histopathology 1988;13:67–78.
39. Powell CD, Paullin TR, Aoisa C, Menzie CJ, Ubaldini A, Westerheide SD. The heat shock transcription factor HSF1 induces ovarian cancer epithelial-mesenchymal transition in a 3D spheroid growth model. PLoS One 2016;11:e0168389.
40. Chen YF, Wang SY, Yang YH, Zheng J, Liu T, Wang L. Targeting HSF1 leads to an antitumor effect in human epithelial ovarian cancer. Int J Mol Med 2017;39:1564–70.
41. Chen YF, Dong Z, Xia Y, Tang J, Peng L, Wang S, et al. Nucleoside analog inhibits microRNA-214 through targeting heat-shock factor 1 in human epithelial ovarian cancer. Cancer Sci 2013;104:1683–9.
42. Yasuda K, Hirohashi Y, Mariya T, Murai A, Tabuchi Y, Kuroda T, et al. Phosphorylation of HSF1 at serine 326 residue is related to the maintenance of gynecologic cancer stem cells through expression of HSP27. Oncotarget 2017;8:31540–53.
43. Autore F, Shanahan CM, Zhang Q. Identification and validation of putative nesprin variants. Methods Mol Biol 2016;1411:211–20.
44. Luo Y, Lee IW, Jo YJ, Namgoong S, Kim NH. Depletion of the LINC complex disrupts cytoskeleton dynamics and meiotic resumption in mouse oocytes. Sci Rep 2016;6:20408.
45. Horn HF, Kim DI, Wright GD, Wong ES, Stewart CL, Burke B, et al. A mammalian KASH domain protein coupling meiotic chromosomes to the cytoskeleton. J Cell Biol 2013;202:1023–39.
46. Esra Demircioglu F, Cruz VE, Schwartz TU. Purification and structural analysis of SUN and KASH domain proteins. Methods Enzymol 2016;569:63–78.
47. Revach OY, Weiner A, Rechav K, Sabanay I, Livne A, Geiger B. Mechanical interplay between invadopodia and the nucleus in cultured cancer cells. Sci Rep 2015;5:9466.
48. Do C, Lang CF, Lin J, Darbary H, Krupska I, Gaba A, et al. Mechanisms and disease associations of haplotype-dependent allele-specific DNA methylation. Am J Hum Genet 2016;98:934–55.
49. Saleh MH, Wang L, Goldberg MS. Improving cancer immunotherapy with DNA methyltransferase inhibitors. Cancer Immunol Immunother 2016;65:787–96.
50. Kijanka G, Murphy D. Protein arrays as tools for serum autoantibody marker discovery in cancer. J Proteomics 2009;72:936–44.